Understanding the rich physics of light propagation in slow photonic crystal waveguides.

Thomas F. Krauss[a], Liam O'Faolain[a], Sebastian Schulz[a], Daryl M. Beggs[a],
Francesco Morichetti[b,c], Antonio Canciamilla[c], M. Torregiani[c] and Andrea Melloni[c]
Simon Mazoyer[d], Phillippe Lalanne[d],
Antonio Samarelli[e], Marc Sorel[e] and Richard De La Rue[e],

[a] University of St Andrews, School of Physics and Astronomy, North Haugh, St Andrews, Fife, KY16 9SS, Scotland.;
[b] POLICOM – DEI Politecnico di Milano, via G. Colombo 81, 20133, Milano, Italy
[c] Fondazione Politecnico di Milano, via Garofalo 39, 20133 Milano, Italy
[d]Laboratoire Charles Fabry de l'Institut d'Optique, CNRS, Univ Paris-Sud, Campus Polytechnique, 91127 Palaiseau cedex, France
[e] Department of Electronics and Electrical Engineering, University of Glasgow, Rankine Building, Oakfield Avenue, Glasgow G12 8LT, Scotland;

ABSTRACT

We study propagation losses in slow light photonic crystal waveguides and show that dispersion engineering can reduce the loss. We develop an improved understanding of why and how this occurs and develop an new approach to modeling these devices that provides new design insights.

Keywords: Photonic Crystal, Slow light

1. INTRODUCTION

Slow light photonic crystal waveguides have a number of promising applications, such as optical delay lines or increased light matter interaction [1-3]. The large refractive index contrast and wavelength scale unit cell provide excellent opportunities for manipulating and controlling light over very short length scales. However, these very same attributes imply that any deviation from the ideal geometry can lead to significant losses, the nature of which is often more complex than appears at first sight.

The W1 waveguide, which consists of a line defect with one row of holes removed from the regular photonic lattice, has long been the workhorse of photonic crystal research. It has already been shown to suffer from significant extrinsic propagation losses in the slow light regime [4,5] with short mean free paths [6]. Clearly, these losses scale inversely with the fabrication technology, so reducing roughness and imperfections is a prime concern. Technology can only be pushed so far, however, so the question arises whether for a given technology, it is possible to reduce the losses by suitable design.

Dispersion engineering [7,8] was developed to modify the parabolic dispersion curve of the W1 waveguide that leads to high group velocity dispersion [9], thus creating a more practical slow light regime. The methods of dispersion engineering typically used also have the effect of shifting the operating regime away from the band edge, a concept that was proposed by O'Faolain et al. as a means of reducing backreflection loss [10]. Dispersion engineered waveguides are already proving to be very successful for nonlinear applications [11,12] as well as delay applications [13]. In this paper, we investigate whether dispersion engineered waveguides also offer improved performance in terms of propagation loss.

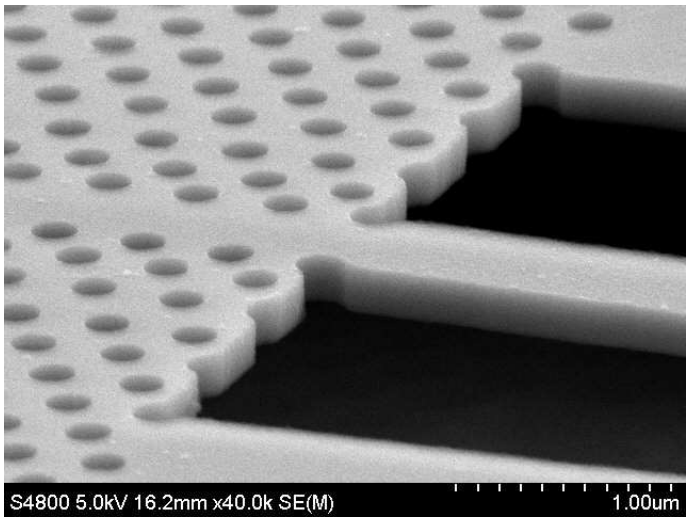

Figure 1. Scanning Electron Microscope image of a dispersion engineered PhC waveguide, highlighting the very smooth and vertical sidewalls.

2. DISPERSION ENGINEERING

Propagating modes in line-defect photonic crystal waveguides are either index-guided, bandgap-guided or guided via a combination of the two. In the latter category, the interaction between the two types of modes causes an anti-crossing which locally alters the shape of the dispersion curve and thus the group velocity of the mode. This suggests a means to control this interaction: bandgap-guiding is predominately affected by the nature of the photonic crystal, whereas the defect governs index guiding - both of which may be controlled independently [7].

The dispersion can also be engineered by laterally shifting the first and second rows of holes adjacent to the defect which alters the form of the anti-crossing [8]. This scheme avoids the necessity for nanometer control over the hole size, which is very difficult to achieve [14], and instead relies on the nanometer positioning of the holes, which is a relatively easy task for electron-beam lithography. Depending on the parameters chosen, the shape of the dispersion curve may be altered so as to reduce the group velocity dispersion. Positional variation of holes is a particularly powerful technique, giving excellent precision and a wide operating range.

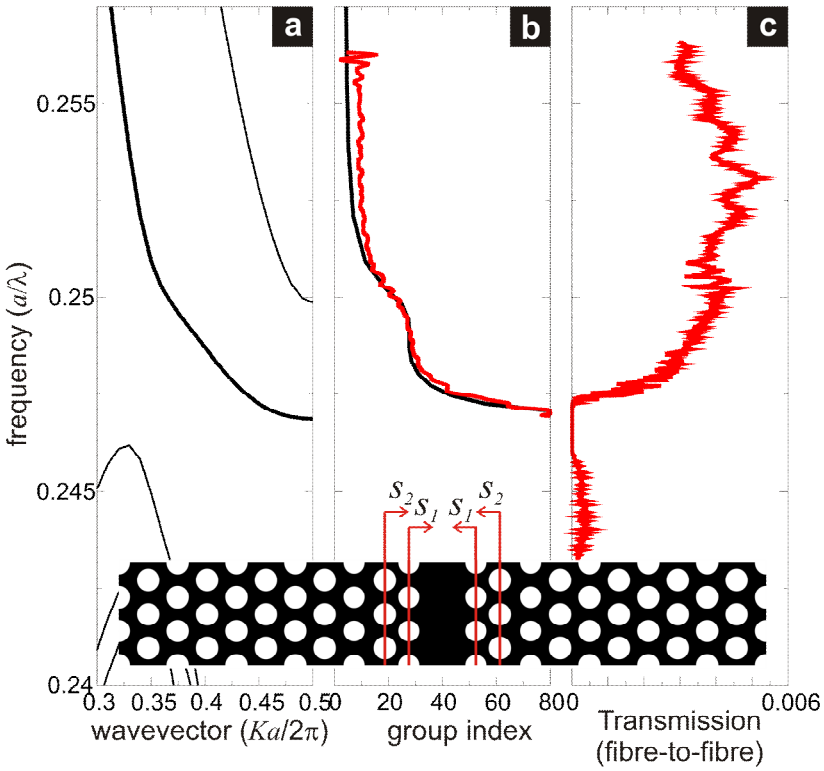

Figure 2. Example of dispersion engineered PhC waveguide for flat-band slow-light based on shifting individual rows of holes. (a) The calculated dispersion relation, with the defect waveguiding mode highlighted in bold. (b) Calculated and measured group index spectra showing the flat-band slow-light at a group index of 25. (c) Measured transmission spectrum. (Inset waveguide length=80um period=410nm) A schematic of the dispersion engineering scheme.

3. FABRICATION AND CHARACTERISATION

The devices were fabricated on a SOITEC silicon-on-insulator wafer, consisting of a 220 nm silicon guiding layer on a 2000 nm layer of buried oxide. The PhC pattern was defined in ZEP-520A electron beam resist using a VISTEC VB6 electron beam writer with a 1.2mm writing field (thereby reducing the effects of stitching errors on the PhC waveguides) operating at 100kV. The pattern was transferred into the silicon layer using reactive ion etching (RIE) with a combination of SF_6 and CHF_3 gas.

Windows defined with photolithography were then opened above the photonic crystal regions and an air bridge created using a hydro-fluoric acid wet etch to selectively remove the SiO_2 buried oxide layer. The fabrication process is based on that of [15], and is known to yield world-class low-loss PhC slab waveguides. Coupling regions, as described in [8,16] were used to aid coupling of light into the slow light regime.

The backscatter measurement was performed by exploiting the interferometric technique described in [17,18]. Light is coupled from a tunable laser into the sample by using lensed fibres and the back-reflected light is extracted by means of an optical circulator and then passed to an optical spectrum analyzer. The polarization of the light is controlled using a polarization scrambler and transverse electric polarization (electric field in the plane of the silicon slab) was measured in this case. By inverse Fourier transforming the measured power spectral density (PSD) of the reflected field, the technique enables to recover in time (space) domain the amplitude and phase of the local backscattering distributed along a generic optical device.

The propagation loss was measured using cutback. The TE-polarization transmission spectrum of each waveguide was measured using a broadband ASE light source and an optical spectrum analyzer. Using a free-space end-fire characterization setup, light was passed through a polarizing beam splitter and coupled into the access waveguides using

microscope objectives. A number of waveguide lengths were measured allowing the loss spectrum to be extracted from a plot of transmission versus length for each wavelength.

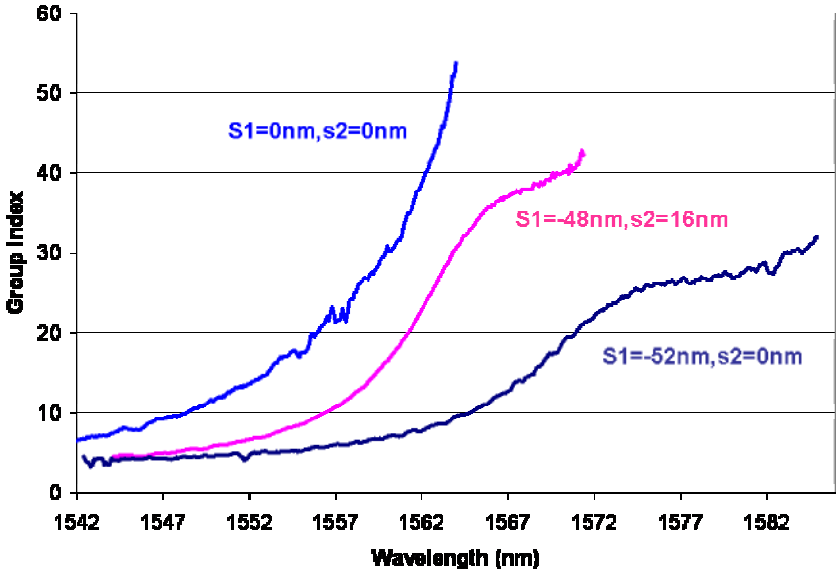

Figure 3. The group index vs wavelength curves of the devices studied in this work. The parameters s1, s2 refer to the relative shift of the first and second row of holes, respectively, as indicated in fig. 1. The s1, s2 = 0 curve refers to the conventional W1 waveguide. For the dispersion engineered waveguides, there is a "plateau" around n_g=37 (pink curve) and ng=26 (black curve). We refer to the beginning of the plateau as the point of inflection, because of the change in curvature. The plateau in these particular samples is less pronounced than designed due to small deviations of the hole sizes from the design values.

The group indices were determined using Fourier transform spectral interferometry. The sample was placed in one arm of a Mach-Zehnder interferometer and the delay recovered from the resulting interference fringes [19].

4. PROPAGATION LOSS- BACKSCATTERING

While photonic crystals operating below the light line are intrinsically lossless, they do exhibit *extrinsic* losses due to fabrication defects, such as sidewall roughness or deviations from the ideal hole position or size that result in the scattering of light. The scattering loss can take two forms, namely a) out of plane scattering, where light is coupled to radiation modes, or b) backscattering, where light is coupled to the counter propagating mode. In the slow light regime, as the density of states in both the forward- and counter- propagating mode increases, the backscattering effect has been shown to scale with n_g^2 [4] or faster [20], which is a serious problem for most applications using slow light in photonic crystals.

To study this phenomenon, the back-reflected light from W1 and slow light engineered PhC waveguides (PhCWs) was measured and compared.

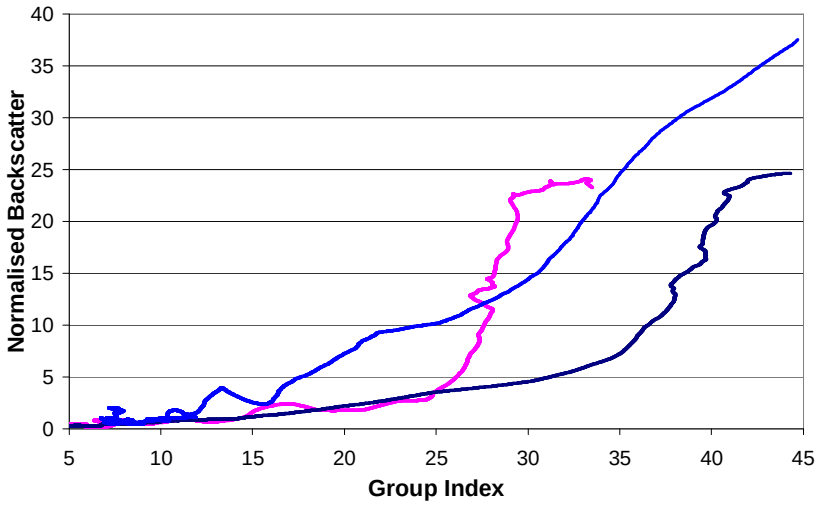

Figure 4. Normalised backscattering signal measurements for 180um long photonic crystal waveguides. For each waveguide the backscattered signal is normalised to that at a group index of $n_g = 5$.

The measurement shows that the backscattering signal for a W1 waveguide (s1=s2=0nm), as studied by Kuramochi et al. [4], can indeed be fitted to a parabola, i.e. it can be shown to scale roughly as n_g^2. This is not the case for the engineered waveguides, however, which exhibit a more complicated functional dependence; here, the initially low backscattering signal increases rapidly after the point of inflection of the group index curve, i.e. in the "plateau" regime.

The measurement technique also provides information about the location of the backreflection source along the sample [17]. Fig. 5 shows a corresponding map of the spatial origin of backscattering signal along a 180-μm long waveguide. On the right of the map are the transmission (blue) and reflection (black) spectra. On the top is the optical path length response resulting from the Fourier transform of the entire 50-nm wide reflection spectrum. Each row of the map is obtained by slicing the Power Spectral Density of the backscattered signal in 4-nm-wide sub-ranges (by using a numerical Gaussian-shaped filter), followed by Fourier transforming this range to yield the optical path length. The operation can also be understood as transforming a frequency window into the time domain, whereby time delay corresponds to optical path length.

The input of the sample is at the left-hand boundary of the map, while the bright line starting at 24 mm from the input at a wavelength of 1530 nm corresponds to the reflection of the output facet of the sample. The physical sample length is approximately L=7.5 mm and the average group index at 1530 nm is around ng=3.5 yielding the measured optical path length of ng*L =24 mm. The shift of the optical path length versus wavelength provides a direct measurement of the increased group index of the PhC waveguide (agreeing well with the technique of [19], indicating that the slow light regime starts above a wavelength of approximately 1550 nm. The end-chip reflection decreases in amplitude as the loss of the sample increases and disappears completely once the wavelength is past the mode cutoff. The high reflection points occurring at 7-mm intervals for wavelengths > 1568nm are caused by multiple round trips of the light in the cavity formed between input facet and the beginning of the photonic crystal which acts as a high reflectivity mirror for wavelengths beyond the mode cutoff.

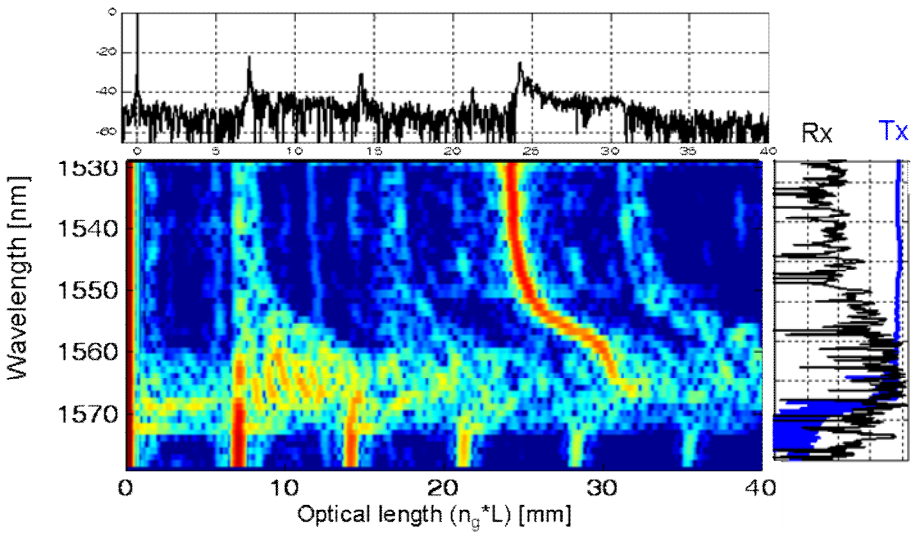

Figure 5. The backscatter map of a 180um long dispersion engineered PhC waveguide (s1=-48nm, s2=16m) The r/a value for this device is slightly different to that in figure 3 resulting in a 7nm shift in wavelength.

From this map, and especially from the resulting reflection and transmission vs wavelength plot on the right hand side, we see that most of the back-reflection occurs within the photonic crystal and that the backscattering level increases for longer wavelengths, where the group index is higher. This allows us to distinguish two regimes: For low group indices (here: ng<35, λ<1565 nm), backscattering only plays a minor role, because the backscattered signal is much lower than the transmitted signal . For higher group indices, the backscattering signal dominates.

5. PROPAGATION LOSS

It is reasonable to assume that propagation loss has an out-of-plane component that scales as n_g, and a backscattering component that scales as n_g^2 [2,4]. This suggests that the loss α in the commonly used Beer-Lambert law, $I(x) = I_0 \exp(-\alpha x)$, needs to be expanded in order to express the loss as a function of group index; the simple form $\alpha \approx n_g^2$ is insufficient. As a first attempt, we may choose $\alpha = \alpha_0 + \alpha_1 n_g + \alpha_2 n_g^2$. Next, we note that the mode shape changes with increased group index [10,20-22]. This change in mode shape is particularly pronounced near the "plateau" of the wavelength-group index plot (fig. 3), which, on closer inspection, corresponds to the point where the confinement mechanism of the mode changes from index guiding to bandgap guiding. The key impact of the mode shape on the losses is that the field concentrates more closely around the perimeter of the holes; since the perimeter is where the imperfections occur, one should indeed use the field on the hole sidewall as an additional parameter in the loss-equation. In figure 6, we calculate the overlap of the mode field with the hole sidewall for a W1 and an engineered photonic crystal waveguide.

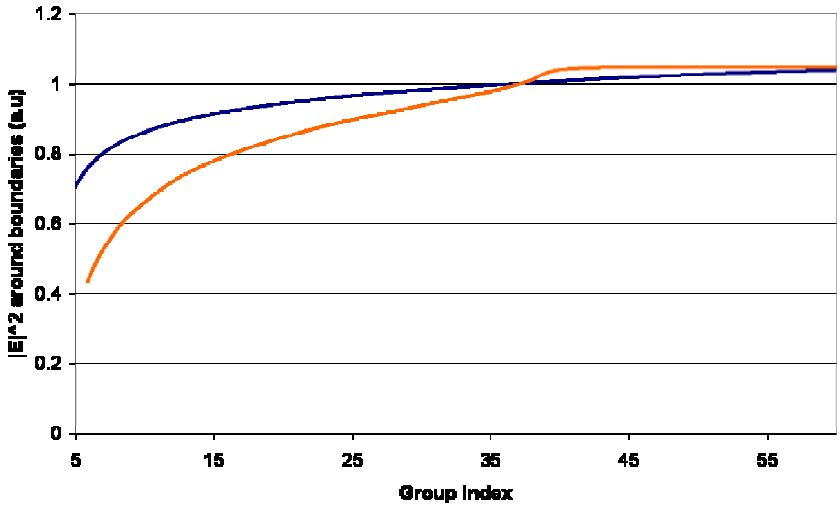

Figure 6: The integral of $|E|^2$ over the hole boundaries. The blue curve was calculated for an unmodified W1 (s1=s2=0) and the red curve for a dispersion engineered PhC waveguide (s1=48nm,s2=-16nm). The calculation was performed using the 3D MIT Photonic-Bands .

At the point of inflection of the n_g curve of the engineered PhCW, (~35-40, see figure 1), there is a step-like change in the overlap value, which causes the corresponding increase in the loss.

Therefore, we can combine all the effects discussed thus far in the following formula,

$$\alpha = \alpha_0 + \alpha_1 n_g \gamma + \alpha_2 n_g^2 \rho \qquad (1)$$

α_0 is the intrinsic loss, which can safely assumed to be zero, while α_1 describes the out-of plane loss and α_2 describes the backscatter loss, and ρ describes the effect of the hole shape. The parameters α_1 and α_2 describe the technological quality of the structures, i.e. sidewall roughness/angle and hole size/position variations; they are independent of the design, so apply irrespective of the structure used, i.e. they are valid both for the W1 and the dispersion engineered waveguide. ρ describes the effects of the mode shape and is a function of n_g.

Following [23] γ, ρ may be expressed as follows:

$$\gamma = \left| \int_{\substack{\text{hole} \\ \text{edges}}} \left(\mathbf{E}_T \cdot \mathbf{E}_T + \frac{1}{\varepsilon} \mathbf{D}_N \cdot \mathbf{D}_N \right) d\mathrm{r} \right| \qquad (2)$$

$$\rho = \left| \int_{\substack{\text{hole} \\ \text{edges}}} \left(\mathbf{E}_T \cdot \mathbf{E}_T + \frac{1}{\varepsilon} \mathbf{D}_N \cdot \mathbf{D}_N \right) d\mathrm{r} \right|^2 , \qquad (3)$$

where $\mathbf{E}_T$ is the electric field tangential to the hole sidewall, $\mathbf{D}_N$ is the electric displacement normal to the hole boundary and the integral is performed over the hole boundary in a unit cell of the photonic crystal. $\mathbf{E}_T$ and $\mathbf{D}_N$ are used to take into account local field corrections and mode shape dispersion.

In figure (7), we plot two different forms of equation 1 for a dispersion engineered PhCW (s1=-48nm, s2=16nm). In green, we use the form that ignores mode shape dispersion (γ=ρ =1 in essence). In red, we plot the form that uses γ and ρ calculated according to equations 2 and 3. The old formulation, in green, gives a reasonable fit for the W1 loss curve- in agreement with previous works [4]- but a very poor fit is very poor for the dispersion engineered PhCWs. For the new version with the correction for the mode shape, in red, the predicted and measured propagation loss are now in good agreement, as seen in Fig 7.

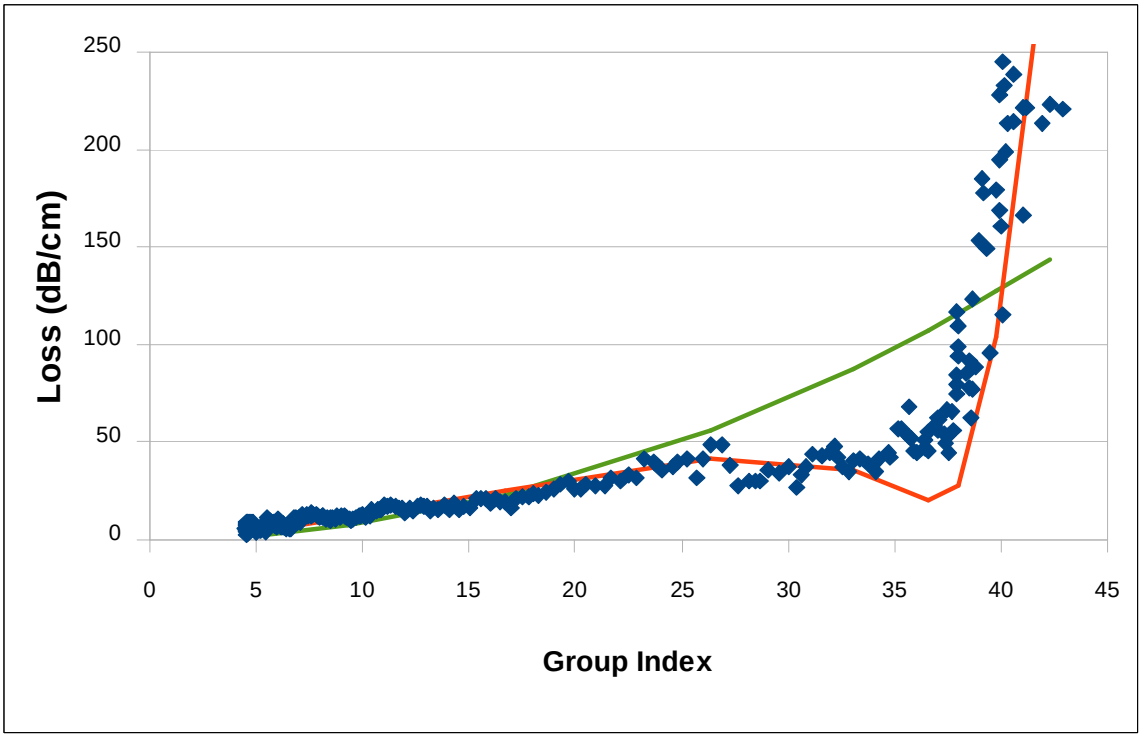

Figure 7: This shows the measured propagation loss(blue diamonds), that predicted using γ=1, ρ=1 (green line) and that given by the new formulation of ρ, (red line). α_1 and α_2 are used as fitting parameters and the same values are used for the different devices (though different for the different forms of the equations). Calculated using MPB (3D).

6. CONCLUSION

We have proposed a new equation that describes propagation loss propagation in photonic crystal waveguides and predict the regions of operation in which this equation if valid. This provides some new insights and gives a new understanding of why dispersion engineering changes the propagation loss.

The transition between the index guided and gap-guided modes (occurring at the point of inflection of the group index curve [21]) is the key factor determining the loss behavior. This transition is best understood through the ρ factor. Before the point of inflection, the mode is distributed such that the value of ρ is low and consequently there is low backscattering. After the point of inflection, there is change in the mode shape that results in a dramatic increase in the value of ρ. This results in a very rapid increase in backscattering.

REFERENCES

1. Krauss T. F., “Slow light in photonic crystal waveguides,” J. App. Phys. D 40, 2666-2670 (2006).
2. Andreani L. C., Gerace D., “Light-matter interaction in photonic crystal slabs,” Phys. Stat. Sol. 234, 3528 (2007)
3. Baba T., “Slow light in photonic crystals,” Nature Photonics 2, 465 (2008).
4. Kuramochi E., Notomi M., Hughes S., Shinya A., Watanabe T. and Ramunno L., “Disorder-induced scattering loss of line-defect waveguides in photonic crystal slabs,” Phys. Rev. B 72, 161318 (2005).
5. Engelen R. J. P., Mori D., Baba T. and Kuipers L., “Two Regimes of Slow-Light Losses Revealed by Adiabatic Reduction of Group Velocity,” Phys. Rev. Lett. 101, 103901 (2008).
6. Wang B., Mazoyer S., Hugonin J. P. and Lalanne P., “Backscattering in monomode periodic waveguides,” Phys. Rev. B 78, 245108 (2008).

7. Frandsen L. H., Lavrinenko A. V., Fage-Pedersen J., and Borel P. I., “Photonic crystal waveguides with semi-slow light and tailored dispersion properties,” Opt. Exp. 14, 9444-9450 (2006).
8. Li J., White T. P., O’Faolain L., Gomez-Iglesias A., Krauss T. F., “Systematic design of flat band slow light in photonic crystal waveguides,” Opt. Exp. 16, 6227-6232, 2008.
9. Engelen R. J. P., Sugimoto Y., Watanabe Y., Korterik J. P., Ikeda N., van Hulst N. F., Asakawa K. and Kuipers L., “The effect of higher-order dispersion on slow light propagation in photonic crystal waveguides,” Optics Expres 14, 1658-1672 (2006).
10. O’Faolain L., White T. P, O’Brien D. , Yuan X., Settle M. D. and Krauss T. F, “Dependence of extrinsic loss on group velocity in photonic crystal waveguides,” Opt. Exp. 15, 13129 (2007).
11. Monat C., Corcoran D., Ebnali-Heidari M., Grillet C., Eggleton B. J., White T. P., O’Faolain L. and Krauss T. F., “Slow light enhancement of nonlinear effects in silicon engineered photonic crystal waveguides,” Opt. Exp. 17, 2944 (2009).
12. Corcoran B., Monat C., Grillet C., Moss D.J., Eggleton B. J., White T.P., O’Faolain L. and Krauss T. F., “Green light emission in silicon through slow-light enhanced third-harmonic generation in photonic-crystal waveguides,” Nature Photonics 3, 206 (2009).
13. O'Faolain L., Schulz S., Beggs D.M., White T.P., Di Falco A., Samarelli A., Sorel M., DeLaRue R.M., Morichetti F., Canciamilla A., Melloni A. and Krauss T. F., “Low loss dispersion engineered photonic crystal waveguides for optical delay lines,” 2009 6th IEEE International Conference on Group IV Photonics, 40-42 (2009). DOI 10.1109/GROUP4.2009.5338297
14. Beggs, D. M., O’Faolain, L., and Krauss, T. F., “Accurate determination of the functional hole size in photonic crystal slabs using optical methods,” Photonics and Nanostructures – Fundamentals and Applications 6, 213-218 (2008).
15. O’Faolain L., Yuan X., McIntyre D., Thoms S., Chong H., De La Rue R. M., and Krauss T. F., “Low-loss propagation in photonic crystal waveguides,” Electron. Lett. 42, 1454-1455 (2006).
16. Hugonin J. P., Lalanne P., White T. P., and Krauss T. F., “Coupling into slow-mode photonic crystal waveguides,” Opt. Lett. 32, 2638-2640 (2007).
17. Morichetti F., Canciamilla A., Ferrari C., Torregiani M., Melloni A., and Martinelli M., “Roughness induced backscattering in optical waveguides,” submitted to Physical Review Letters.
18. Morichetti F., Melloni A., Canciamilla A., Samarelli A., Sorel M., De La Rue R. M., and Martinelli M., “Coherent backscattering in optical microring resonators,”submitted to Optics Letters.
19. Gomez-lglesias A, O’Brien D., O’Faolain L., Miller A., and Krauss T. F., “Direct measurement of the group index of photonic crystal waveguides via Fourier transform spectral interferometry,” Appl. Phys. Lett. 90, 261107 (2007).
20. Mazoyer S., Hugonin J. P., and Lalanne P., “Disorder-Induced Multiple Scattering in Photonic-CrystalWaveguides”, Phys. Rev. Lett, 103, 1063903 (2009)
21. Petrov A., Krause M., and Eich M., “Backscattering and disorder limits in slow light photonic crystal waveguides,” Opt. Express 17, 8676 (2009).
22. Patterson M., Hughes S., Schulz S., Beggs D. M., White T. P., O’Faolain L., and Krauss T. F., “Disorder-induced incoherent scattering losses in photonic crystal waveguides: Bloch mode reshaping, multiple scattering, and breakdown of the Beer-Lambert law,” Phys. Rev. B 80, 195305 (2009).
23. G. Lecamp, J. P. H. & Lalanne, P. “Theoretical and computational concepts for periodic optical waveguides,” Optics Express 15, 11042-11060 (2007).